Fabrication and Characterization of Advanced Triple-junction Amorphous Silicon Based Solar Cells

PHASE I – Quarter 4

Quarterly Technical Progress Report

December 1, 2005 to February 28, 2006

NREL Subcontract No. ZXL-5-44205-06

Subcontractor: The University of Toledo

Principal Investigator: Xunming Deng
(419) 530-4782; dengx@physics.utoledo.edu

Co-Principal Investigator: Robert W. Collins
(419) 530-2195; rcollins@physics.utoledo.edu

Department of Physics and Astronomy
University of Toledo, Toledo, OH 43606

Contract technical monitor: Dr. Bolko von Roedern

Table of Contents

Section 1

Executive Summary

This quarterly technical progress report covers the highlights of the research activities and results on the project of "The Fabrication and Characterization of High-efficiency Triple-junction a-Si Based Solar Cells" at the University of Toledo for the Period of December 1, 2005 to February 28, 2006, under NREL TFPPP subcontract number ZXL-5-44205-06.

Following this Executive Summary are two sections describing research performed during this quarter related to the tasks under this subcontract. The major technical progresses of these sections are summarized as follows:

Section 2: Fabrication and Optimization of Amorphous Silicon Based Triple-junction Solar Cell with Nanocrystalline Silicon Bottom Cell

Using VHF PECVD technique, new deposition regimes have been developed in our UT multi-chamber load-locked PECVD deposition system for the preparation of high quality a-Si:H, a-SiGe:H and nc-Si:H i-layers at deposition rates in the range of 2-15 Å/s. Incorporating various improvements in device fabrication and characterization, 7.8% initial and 7.4% stable active-area (0.25 cm^2) cell efficiencies have been achieved for VHF nc-Si n-i-p single-junction solar cells. Using nc-Si:H cell as component bottom-cell, 12.4% initial and 11% stable cell efficiencies in a-Si/a-SiGe/nc-Si triple-junction structure have also been achieved. In the next period, we will incorporate real-time spectroscopic ellipsometry (RTSE) into the triple-junction cell fabrication system to determine phase diagrams for a-Si, a-SiGe and nc-Si i-layers. With a better understanding of the processes, improvements in efficiencies are expected.

Section 3: Roughness and Phase Evolution in $Si_{1-x}Ge_x$:H from Real Time Spectroscopic Ellipsometry: Guidance for Multijunction Photovoltaics

In this study, a-$Si_{1-x}Ge_x$:H films have been prepared by rf PECVD on the cathode (V_b ~ 20 V) in order to track the effects of increased Ge concentration and H_2-dilution on film microstructural evolution and predicted material characteristics. Through such studies, it is shown that the R value at which the amorphous-to-mixed phase transition occurs for the desired device thickness increases with increasing G. Optimum alloy fabrication just before the amorphous-to-mixed phase transition for the given thickness is demonstrated through the minimum stable surface roughness and the maximum amorphous roughening transition for materials with optical (Tauc) band gaps from 1.85 to 1.35 eV and below. A simple depiction is provided detailing the continuous improvements in material properties accessible by increasing R to the mixed-phase boundary.

Section 2

Fabrication and Optimization of Amorphous Silicon Based Triple-junction Solar Cell with Nanocrystalline Silicon Bottom Cell

Xinmin Cao, Wenhui Du, Xunming Deng
Department of Physics and Astronomy, University of Toledo, Toledo, OH 43606, USA

ABSTRACT

Using VHF PECVD technique, new deposition regimes have been developed in our UT multi-chamber load-locked PECVD deposition system for the preparation of high quality a-Si:H, a-SiGe:H and nc-Si:H i-layers at deposition rates in the range of 2-15 Å/s. Incorporating various improvements in device fabrication and characterization, 7.8% initial and 7.4% stable active-area (0.25 cm^2) cell efficiencies have been achieved for VHF nc-Si n-i-p single-junction solar cells. Using nc-Si:H cell as component bottom-cell, 12.4% initial and 11% stable cell efficiencies in a-Si/a-SiGe/nc-Si triple-junction structure have also been achieved.

1. Introduction

In recent years, nc-Si:H (μc-Si:H) solar cell, which has a better light soaking stability than a-Si:H and a-SiGe:H solar cells[1], becomes one of the essential highlights in silicon based thin-film Photovoltaic research and production in the world. Incorporating nc-Si:H cell as bottom cell, a-Si:H/nc-Si:H and a-Si:H/a-SiGe:H/nc-Si:H multi-junction cells with efficiencies exceeding 13% have been successfully obtained by several groups[2-5]. Based on our previous research work of a-Si based solar cells[6] and using the Si:H phase diagrams[7], we have expanded our research area from a-Si:H/a-SiGe:H and a-Si:H/a-SiGe:H/a-SiGe:H multi-junction solar cells with a-SiGe:H bottom cell to a-Si:H/nc-Si:H and a-Si:H/a-SiGe:H/nc-Si:H multi-junction cells using nc-Si:H as the bottom cell, which is based on the project "The Fabrication and Characterization of High-efficiency Triple-junction a-Si Based Solar Cells" at the University of Toledo (UT) under the NREL TFPP Program.

2. Experimental

a-Si:H, a-SiGe:H, and nc-Si:H single-junction solar cells, and a-Si:H/a-SiGe:H/nc-Si:H triple-junction solar cells were fabricated using our UT nine-chamber PECVD/Sputtering cluster tool system. This system, with four PECVD chamber for silicon thin films, four sputter chambers for Al/Ag/ZnO and ITO, and one chamber for load-lock, all connected together by gate valves, allows researcher at UT to fabricate 4"x 4" silicon thin-film solar cells with different structures without vacuum break. Both the doped n-layers and the doped p-layers were prepared using the conventional 13.56 MHz RF-PECVD technique at deposition rates of 1-2 Å/s. Using the VHF-PECVD technique with a frequency of 70 MHz, the preparation of high quality a-Si:H, a-SiGe:H and nc-Si:H i-layers were made with a low pressure of 0.1-0.5 Torr at deposition rates in the range of 2-15 Å/s. After fabrication of the nip structures, the cells were completed with a mask by depositing Indium Tin Oxides (ITO) transparent conductive layers as front contacts using standard RF sputter deposition techniques. Each cell has an active area of 0.25 cm^2. The as-deposited cells were evaluated using IV measurement with an AM1.5 solar simulator. Quantum efficiency measurement was made in the wavelength range of 350 – 1000 nm. Light soaking was taken under one sun light with cell temperature being at 50 °C. The data of short-circuit current density J_{sc}, open-circuit voltage V_{oc}, fill factor FF and QE of these cells were compared and analyzed for the device performances.

3. Results and Discussions

3.1 a-Si,a-SiGe and nc-Si single-junction solar cells

High quality a-Si, a-SiGe and nc-Si i-layers have been developed using VHF PECVD technique in new deposition regimes at deposition rates in the range of 2-15 Å/s. Their corresponding device performances have been evaluated using n-i-p single-junction structure on SS/Ag/ZnO substrates. The n-layer and p-layer depositions have also been optimized for each i-layer. Table 1 lists the representative IV data of a-Si, a-SiGe and nc-Si single-junction cells. With deposition rates near 3 Å/s, a-Si cell has an initial efficiency of η = 9.3% with an i-layer thickness of 160 nm and a-SiGe cell has an initial efficiency of 10.4% with an i-layer thickness of 180 nm. nc-Si cells with initial efficiencies of 6.6% and 7.8% have been obtained at deposition rates of r_{dep} = 10 Å/s and r_{dep} = 3 Å/s, respectively. IV and QE curves of the VHF nc-Si cell with an i-layer deposition rate near 3 Å/s and thickness of 1750 nm are also shown in Fig 1 and Fig.2

Table 1. IV data of a-Si, a-SiGe and nc-Si cells..

Cell	i-layer r_{dep}(Å/s)	i-layer t (min)	V_{oc} (V)	J_{sc} (mA/cm^2)	FF	η (%)
a-Si	3	9	0.969	13.4	0.72	9.3
a-SiGe	3	10	0.813	19.5	0.66	10.4
nc-Si #1	10	25	0.453	21.3	0.68	6.6
nc-Si #2	3	100	0.529	22.3	0.66	7.8

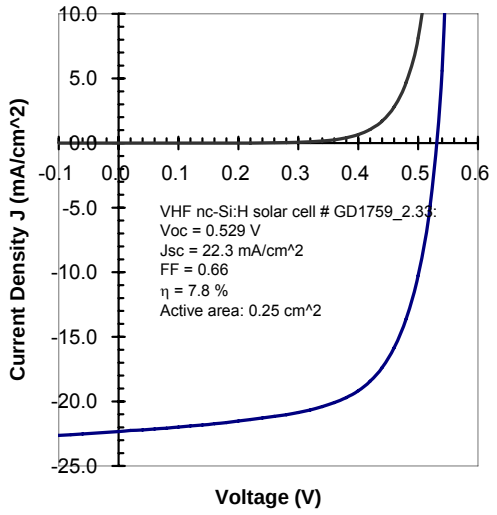

Fig. 1. IV curve of an UT fabricated VHF nc-Si:H n-i-p single-junction solar cell at a deposition rate of 3 Å/s.

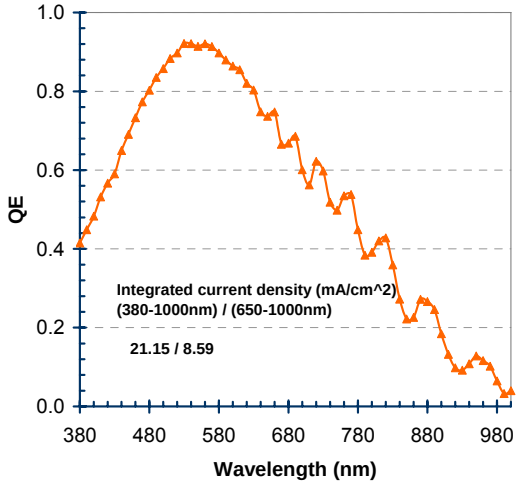

Fig. 2. QE curve of an VHF nc-Si:H solar cell whose IV data is shown in Fig 1.

3.2 a-Si:H/a-SiGe:H/nc-Si:H triple-junction solar cells

As displayed in Table 2, an initial efficiency of η=10.3% for the triple-junction cell (tri-cell C1) which is composed of component RF a-Si top-cell, RF a-SiGe mid-cell and VHF nc-Si bot-cell has been obtained. An initial efficiency of η=11.0% for VHF a-Si:H/a-SiGe:H/nc-Si:H triple-junction cell (tri-cell C2) was also achieved. The deposition time of the tri-cell C2 has been greatly reduced, while its efficiency is kept in the same range as C1.

The tri-cell C3 was made by using VHF 3Å/s nc-Si:H bot-cell with an i-layer thickness of 1250 nm. The top-cell and mid-cell for tri-cell C3 has been further optimized based on the tri-cell C2. The J_{sc} value of the tri-cell C3 is limited by nc-Si bottom-cell. The V_{oc} and FF values for C3 increased and an initial active-area ($0.25cm^2$) efficiency of 12.4% was reached. The IV and QE curves for the tri-cell C3 are shown in Fig. 3 and Fig. 4, respectively.

As also listed in Table 2, after 100 hours of light soaking, the efficiency of the tri-cell C3 was dropped from 12.4% to 11.0%. There was no further light-induced degradation for C3 under long-term light soaking. The most loss was in the first 100 hrs of light soaking. After 1000 hrs of light soaking, C3 has a stable efficiency of 11.0% (V_{oc}= 2.116V, J_{sc}=7.38 mA/cm^2 and FF=0.704).

Table 2. IV data of a-Si/a-SiGe/nc-Si cells..

Triple-cell No.	structure	i-layer t (min)	V_{oc} (V)	J_{sc} (mA/cm^2)	FF	η (%)
C1 initial	RF a-Si top-cell	85	2.132	7.23	0.672	10.3
	RF a-SiGe mid	60				
	VHF nc-Si bot	25				
C2 initial	VHF a-Si top-cell	9	2.098	7.61	0.691	11.0
	VHF a-SiGe mid	14				
	VHF nc-Si bot	28				
C3 initial	VHF a-Si top	14	2.183	7.55	0.752	12.4
	VHF a-SiGe mid	25				
	VHF nc-Si bot	60				
C3 100 hrs of light soaking			2.138	7.29	0.702	11.0
C3 1000 hrs of light soaking			2.116	7.38	0.704	11.0

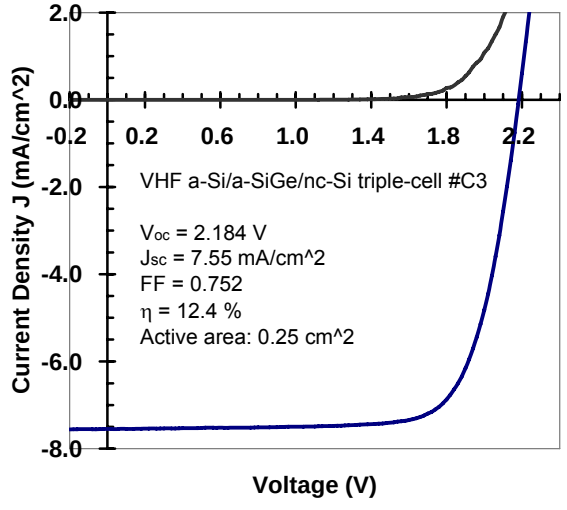

Fig. 3. IV curve of the VHF a-Si/a-SiGe/nc-Si triple cell C3 at a deposition rate of 3 Å/s.

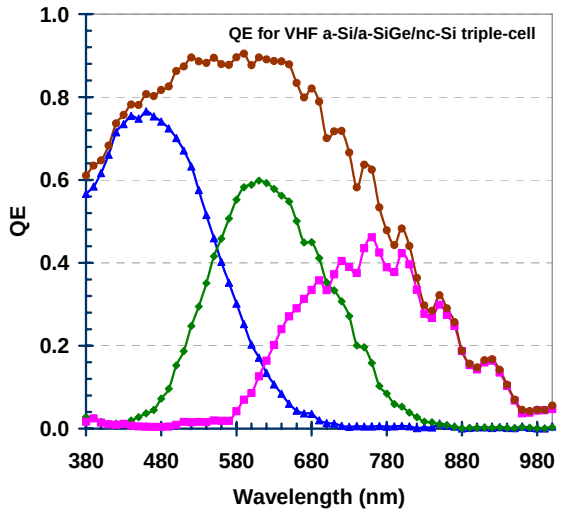

Fig. 4. QE curve of the VHF a-Si/a-SiGe/nc-Si triple cell C3 whose IV data is shown in Fig 3.

4. Summary

A report of fabrication and characterization of a-Si, a-SiGe and nc-Si single-junction, and a-Si/a-SiGe/nc-Si triple-junction solar cells of good performances using VHF PECVD is presented. In the next period, we will incorporate real-time spectroscopic ellipsometry (RTSE) into the triple-junction cell fabrication system to determine phase diagrams for a-Si, a-SiGe and nc-Si i-layers. With a better understanding of the processes, improvements in efficiencies are expected.

ACKNOWLEDGEMENTS

Work was supported by NREL TFPPP under subcontract no. ZXL-5-44205-06.

REFERENCES

[1] A.V. Shah, J. Meier, E. Vallat-Sauvain, N. Wyrsch, U. Kroll, C. Droz, and U. Graf, "Material and solar cell research in microcrystalline silicon", *Solar Energy Materials & Solar Cells* **78**, 469 (2003).

[2] B. Yan, G. Yue, J. Yang, and S. Guha, *Applied Physics Letters* **85**, 1955 (2004).

[3] J. Meier, J. Spitznagel , U. Kroll , C. Bucher , S. Fay , T. Moriarty, and A. Shah, *Thin Solid films* **451-452**, 518 (2004).

[4] K. Yamamoto, A. Nakajima, M. Yoshimi, T. Sawada, S. Fukuda, T. Suezaki, M. Ichikawa, Y. Koi, M. Goto, H. Takata, T. Sasaki, and Y. Tawada, *Proc. of 3rd World Conf. on Photovoltaic Energy Conversion*, Osaka, Japan, May, 2003.

[5] K. Saito, M. Sano, H. Otoshi, A. Sakai, S. Okabe, and K. Ogawa, *Proc. of 3rd World Conf. on Photovoltaic Energy Conversion*, Osaka, Japan, May, 2003.

[6] X. Deng, "Optimization of a-SiGe based triple, tandem and single-junction solar cells", *31st IEEE Photovoltaic Specialist Conference,* Orlando, Florida, January, 2005.

[7] R. W. Collins, A. S. Ferlauto, G. M. Ferreira, C. Chen, J. Koh, R.J. Koval, Y. Lee, J. M. Pearce, C. R. Wronski, *Solar Energy Materials & Solar Cells* **78**, 143 (2003).

Section 3

Roughness and Phase Evolution in $Si_{1-x}Ge_x$:H from Real Time Spectroscopic Ellipsometry: Guidance for Multijunction Photovoltaics

N. J. Podraza and R. W. Collins

Department of Physics and Astronomy, University of Toledo, Toledo, OH 43606

Overview

The surface roughness and phase evolution of hydrogenated silicon-germanium alloys ($Si_{1-x}Ge_x$:H), prepared by rf plasma-enhanced chemical vapor deposition (PECVD) on crystalline Si substrates held at 200°C, have been studied using real time spectroscopic ellipsometry (RTSE). These alloy films were deposited under cathodic bias conditions (V_b ~ −20 V) at different GeH_4 and H_2 flow ratios $G=[GeH_4]/\{[SiH_4]+[GeH_4]\}$ and $R=[H_2]/\{[SiH_4]+[GeH_4]\}$, respectively, in order to track the effects of these ratios on film microstructural evolution and predicted material characteristics (based on previous extensive correlations). Through such studies, the three dimensional nature of parameter space is revealed, whereby it is shown that the R value at which the amorphous-to-mixed phase transition occurs for the desired device thickness -- and thus, the optimum condition for alloy fabrication -- increases with increasing G. A simple depiction is provided of the continuous improvements in material properties accessible by increasing R.

Introduction

Optimization of the a-Si:H i-layer component of the top cell has been widely successful by applying the concept of maximum H_2 dilution. This concept has been applied in both two-step and multistep processing in order to achieve the greatest benefits of atomic H, while suppressing microcrystallite evolution. The resulting protocrystalline nature of the i-layer leads to the highest device performance and stability. Under such PECVD conditions, Si:H depositions on smooth, oxidized c-Si substrates exhibit the largest and most rapid smoothening during coalescence, the smoothest stable surface, as well as the largest thickness at which a roughening onset occurs in the amorphous growth regime. The applicability of the maximum dilution concept for $Si_{1-x}Ge_x$:H alloys is alos of interest. For these latter alloys, however, more detailed studies are required with an ultimate goal of improving the photovoltaic properties of higher deposition rate materials. In this study, the growth processes for $Si_{1-x}Ge_x$:H alloys have been investigated using RTSE. The goal is to develop deposition phase diagrams that provide a clearer roadmap for optimization of the alloys in photovoltaic applications by applying general principles. With this approach, potential directions for improvements in multijunction cells may be identified that may have been overlooked in previous optimizations.

Experimental Details

The $Si_{1-x}Ge_x$:H films for phase diagram development were deposited on native-oxide/c-Si using single-chamber rf (13.56 MHz) PECVD and were measured in real time using a rotating-compensator multichannel ellipsometer. For all depositions performed as a function of the phase diagram parameter $R=[H_2]/\{[SiH_4]+[GeH_4]\}$, conventional PECVD conditions from pure Si:H PECVD were adopted for the most part, including a relatively low substrate temperature (T = 200°C), the minimum plasma power possible for a stable plasma (0.08 W/cm^2), a low partial pressure of the source gases $\{[SiH_4]+[GeH_4]\}$ (~ 0.06 Torr), and a low total pressure (< 1.0 Torr). In contrast to conventional Si:H PECVD, however, the substrates for $Si_{1-x}Ge_x$:H deposition in this study were placed on the cathode where the self-bias was $V_b \sim -20$ V. The flow ratio $G = [GeH_4]/\{[SiH_4]+[GeH_4]\}$ was varied from G=0 to G=0.167.

Results and Discussion

Figure 1 shows basic deposition and materials information for the films with R=10 studied here. Figure 1(a) shows the growth rates of the R=10 films deposited at different G from 0.0 up to 0.167. Figure 1(b) shows the Ge concentration, x, as a function of G, as determined by x-ray photoelectron spectroscopy (XPS).

Figure 2 shows the surface roughness evolution of a series of films prepared under identical conditions with fixed R=10, while G varied from 0.0 up to 0.167. The surface roughness evolution demonstrates a decrease in the bulk layer thickness at which the amorphous roughening transition [a → a] occurs with increasing G. For G=0, this transition occurs at a bulk layer thickness, d_b=3400 Å, whereas for G=0.167 this transition occurs at only d_b=220 Å. Additionally, prior to the amorphous roughening transition these films pass through a stable

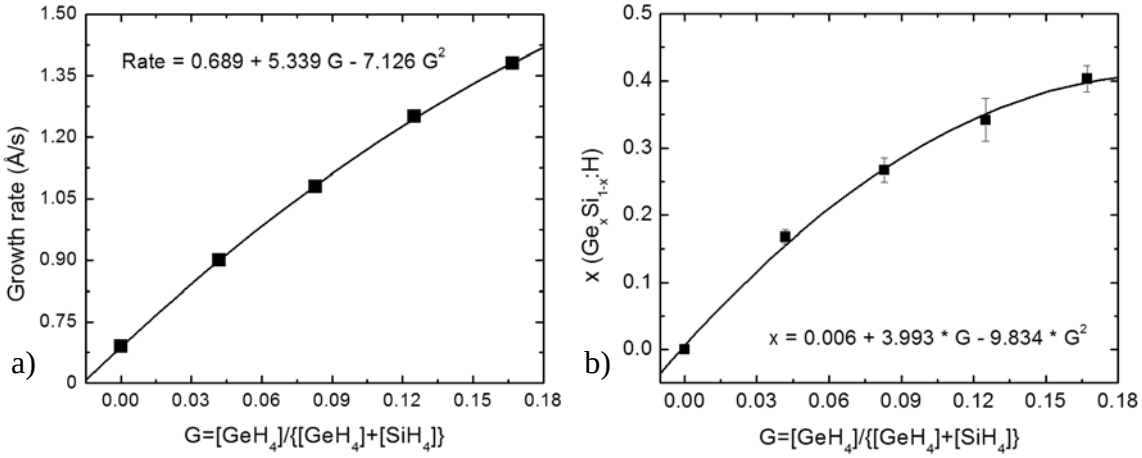

Fig. 1 (a) Growth rate and (b) Ge concentration x for a series of a-$Si_{1-x}Ge_x$:H films prepared under rf PECVD conditions that include: a substrate temperature of T=200°C, a total pressure of p<1 Torr, an rf power of P=0.08 W/cm^2, a cathodic dc bias of $V_b \sim -20$V, and fixed H_2 dilution ratio R=10. The films compared were prepared at varying GeH_4

dilution ratios conditions, represented by $G=[GeH_4]/\{[GeH_4]+[SiH_4]\}$, with $0.0 \leq G \leq 0.167$.

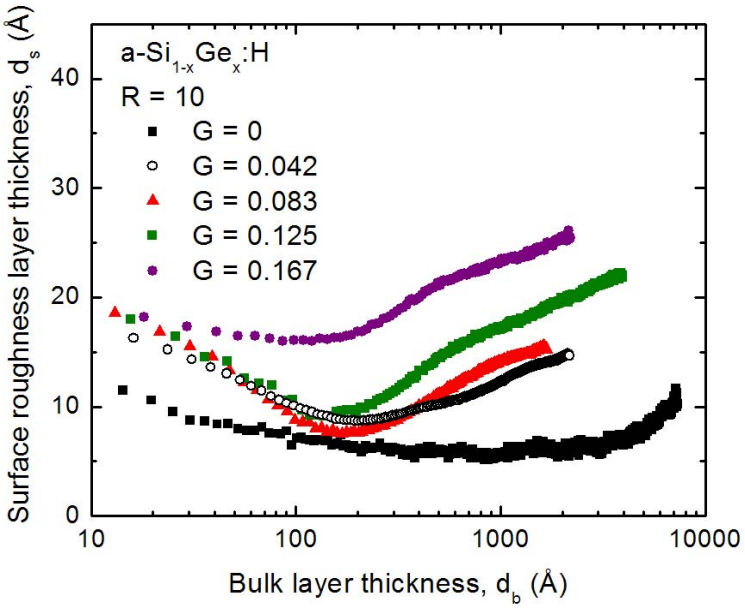

Fig. 2 Surface roughness evolution for a series of $a\text{-}Si_{1-x}Ge_x\text{:}H$ films prepared under rf PECVD conditions that include: a substrate temperature of T=200°C, a total pressure of p<1 Torr, an rf power of P=0.08 W/cm^2, a cathodic dc bias of $V_b \sim -20V$, and fixed H_2 dilution ratio R=10. The films compared were prepared at varying GeH_4 dilution ratios conditions, represented by $G=[GeH_4]/\{[GeH_4]+[SiH_4]\}$, with $0.0 \leq G \leq 0.167$.

surface regime. In this stable surface regime, the roughness layer thickness increases with increasing G, from $d_s \sim 5$ Å at G=0 to $d_s \sim 17$ Å at G=0.167. These two trends demonstrate the expected decrease in film quality with G.

Figure 3 (solid line) shows the rapid reduction in the a→a transition continuously versus G at fixed R=10. This deterioration can be minimized by increasing R progressively with increasing G so as to operate at maximum R without crossing the [a→(a+μc)] transition for the desired thickness of the solar cell i-layer. This process is demonstrated by the upward arrow, and the broken line boundary for the amorphous roughening transition represents an envelope of the optimum depositions as a function of G, allowing for variations in R. Figure 4 provides a sample comparison of two G=0.167 films prepared at relatively low H_2 dilution (R=10) and the maximal H_2 dilution without the [a → (a+μc)] transition occurring (R=90). These films show that by increasing R, even at G=0.167, the [a → a] transition can be shifted up to d_b=1670 Å at R=90, and the stable surface roughness thickness can be reduced to ~ 7 Å, both of which indicate significant improvements in film quality. As noted in Fig. 4, linear extrapolation of $\varepsilon_2^{1/2}$ at the deposition temperature (T=200°C) shows that the Cody-Lorentz band gap of these materials increases somewhat with increased H_2 dilution.

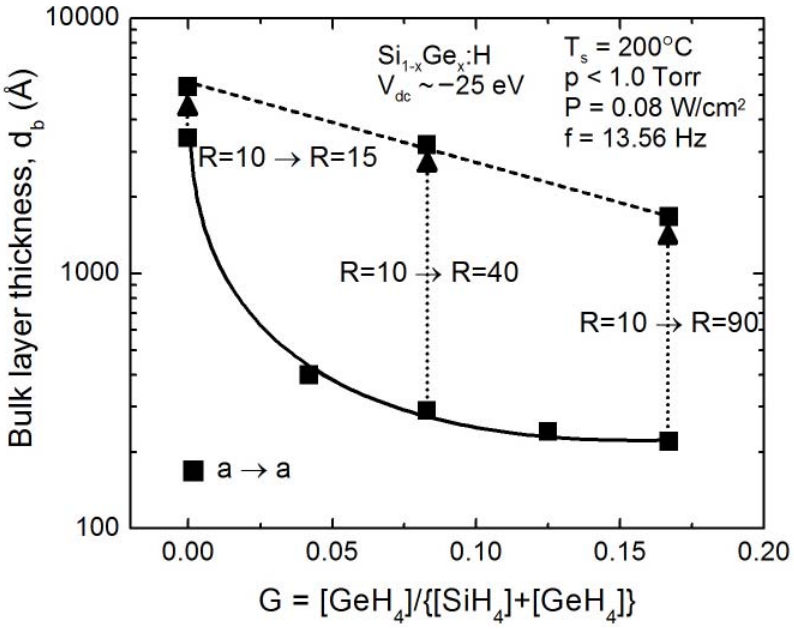

Fig. 3 A single deposition phase diagram for R= 10 $Si_{1-x}Ge_x$:H films plotted versus the GeH_4 flow ratio G. The thicknesses of the amorphous roughening transition (solid line and square points) are depicted. The dotted arrows represent the increase in the amorphous roughening transition possible with the increase in R indicated, i.e., up to the amorphous-to-(mixed-phase) transition for a thick film.

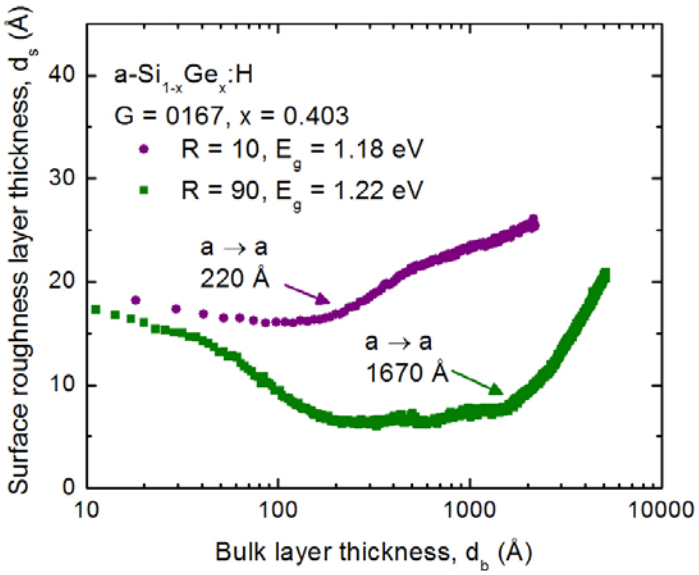

Fig. 4 Surface roughness evolution for a pair of a-$Si_{1-x}Ge_x$:H films prepared under conditions as described above with fixed G=0.167. The two films compared were prepared at H_2 dilution ratios of R=10 (circles) and R=90 (squares). The amorphous roughening transition shifts from 220 Å at R=10 to 1670 Å at R=90, while the Cody-Lorentz band gaps obtained from extrapolation of $\varepsilon_2^{1/2}$ at the deposition temperature of 200°C shifted from 1.18 eV to 1.22 eV.

Summary

In this study, a-$Si_{1-x}Ge_x$:H films have been prepared by rf PECVD on the cathode (V_b ~ −20 V) in order to track the effects of increased Ge concentration and H_2-dilution on film microstructural evolution and predicted material characteristics. Through such studies, it is shown that the R value at which the amorphous-to-mixed phase transition occurs for the desired device thickness increases with increasing G. Optimum alloy fabrication just before the amorphous-to-mixed phase transition for the given thickness is demonstrated through the minimum stable surface roughness and the maximum amorphous roughening transition for materials with optical (Tauc) band gaps from 1.85 to 1.35 eV and below. A simple depiction is provided detailing the continuous improvements in material properties accessible by increasing R to the mixed-phase boundary.

Acknowledgments

The authors acknowledge the contributions of Professor C. R. Wronski to this work.